Intermediate Model Solutions to the Lorenz Equations: Strange Attractors and Other Phenomena

PETER R. GENT AND JAMES C. MCWILLIAMS

National Center for Atmospheric Research,[1] Boulder, CO 80307

(Manuscript received 13 April 1981, in final form 21 July 1981)

ABSTRACT

The low-order, nine-component, primitive equation model of Lorenz (1980) is used as the basis for a comparative study of the quality of several intermediate models. All the models are intermediate between the primitive equations and quasi-geostrophy and will not support gravity-wave oscillations; this reduces to three the number of independent components in each. Strange attractors, stable limit cycles, and stable and unstable fixed points are found in the models. They are used to make a quantitative intercomparison of model performance as the forcing strength, or equivalently the Rossby number, is varied. The models can be ranked from best to worst at small Rossby number as follows: the primitive equations, the balance equations, hypogeostrophy, geostrophic momentum approximation, the linear balance equations, and quasi-geostrophy. At intermediate Rossby number the only change in this ranking is the demotion of hypogeostrophy to the position of worst. Caveats about the low-order model, and hence the generality of the conclusions, are also discussed.

1. Introduction

Intermediate models, those between the primitive equations and quasi-geostrophy, are discussed extensively in McWilliams and Gent (1980). It is noted in that paper that there are few intermediate model solutions available that can be used for quantitative comparisons (n.b., the steady circular flow solutions discussed therein are highly idealized). A severely truncated, low-order primitive equation model, which has just nine independent components, is discussed in Lorenz (1980). It is complicated enough to have interesting behavior—strange attractors, stable limit cycles, and stable and unstable fixed points—yet requires only a modest effort in numerical model development and takes a trivial amount of computation time. We found that the model also is complicated enough so that all the intermediate models give different equations and solutions, which is not the case for steady circular flow. However, the quasi-geostrophic version of the model, which is discussed also by Lorenz (1963, 1980) and has only three independent components, is simple enough that some of its properties can be determined analytically. Thus we decided the Lorenz model is appropriate for a quantitative comparison of the quality of its intermediate model solutions that is neither trivial nor very demanding of modeling resources. Lorenz (1980) made a detailed examination of the attractor set topologies for the primitive equations and quasigeostrophy, but we have not done this comprehensively for the intermediate models. Rather, we have used the grosser measure of the transitions between different regimes of behavior for the model intercomparison instead of the more subtle differences between attractor set topologies which are more difficult to describe concisely. We have no doubts that the intermediate model attractor set topologies lie between, or at least close to, the two extremes explored by Lorenz.

The low-order Lorenz primitive equation (PE) model is reviewed and then the low-order form of the intermediate model equations are given in Section 2. The intermediate models discussed are the balance equations (BE), the geostrophic momentum approximation (GM), the hypogeostrophic equations (HG), and the linear balance equations (LBE). In addition, we include quasigeostrophy (QG). The LBE are the only member of this set not discussed in McWilliams and Gent (1980). The LBE use the linear form of the truncated BE divergence equation to relate the streamfunction of the rotational velocity component to the geopotential. The vorticity equation is also further truncated from the BE form in the appropriate manner such that an energy conservation principle is retained (see Lorenz, 1960). The various methods to solve the intermediate model equations are described in Section 3, and Section 4 contains the model comparisons. Two caveats about the generality of our comparison are discussed in Section 5. The first is the fact that, except in the case of quasigeostrophy, the low-order models do not have

[1] The National Center for Atmospheric Research is sponsored by the National Science Foundation.

0022-4928/82/010003-11$06.75

an energy conservation principle (even for those continuous intermediate models that possess them). The second is that, as the forcing or Rossby number is reduced, the asymptotic convergence between PE, intermediate models, and QG is extremely slow in certain parameter ranges. Finally, Section 6 contains our conclusions.

2. The models

a. *Primitive equations (PE)*

The primitive equation model and the low-order truncation are exactly as in Lorenz (1980) and will only be briefly reviewed here. The model is a form of the shallow-water equations governing hydrostatic, homogeneous, incompressible, uniformly rotating flow of infinite horizontal extent moving over topography $h(\mathbf{r})$. The upper free surface of the fluid is at height $H + z(\mathbf{r})$, where the horizontal averages of z and h are zero. The horizontal velocity $\mathbf{V}(t, \mathbf{r})$ is independent of height and the vertical velocity is determined from mass continuity. The flow is forced by a mass source $F(\mathbf{r})$ and is damped diffusively with coefficients ν and κ.[2] The governing equations are

$$\left(\frac{\partial}{\partial t} + \mathbf{V}\cdot\nabla\right)\mathbf{V} + f\mathbf{k}\times\mathbf{V} = -g\nabla z + \nu\nabla^2\mathbf{V}, \quad (1)$$

$$\left(\frac{\partial}{\partial t} + \mathbf{V}\cdot\nabla\right)(z-h) + (H + z - h)\nabla\cdot\mathbf{V} = F + \kappa\nabla^2 z, \quad (2)$$

where g is the gravitational acceleration and $\mathbf{k}$ is a unit vertical vector. The horizontal velocity is split into its rotational and divergent components by defining

$$\mathbf{V} = \mathbf{k}\times\nabla\psi + \nabla\chi. \quad (3)$$

Equations for the vorticity $\nabla^2\psi$ and the divergence $\nabla^2\chi$ are given in Lorenz (1980).

The low-order model consists of introducing three horizontal wavenumber vectors, α_1, α_2 and α_3, which sum to zero, and the corresponding orthogonal functions

$$\phi_i = \cos(\alpha_i\cdot\mathbf{r}/L), \quad i = 1, 2, 3, \quad (4)$$

where L is a horizontal length scale. All model variables are assumed to be sums of these basis functions ϕ_i and those parts of the nonlinear terms which do not project onto the basis functions are ignored. For i, j and k in cyclic order, constants can be defined as

$$\left.\begin{aligned} a_i &= \alpha_i\cdot\alpha_i \\ b_i &= \alpha_j\cdot\alpha_k = \tfrac{1}{2}(a_i - a_j - a_k) \\ c_i &= \alpha_j\times\alpha_k\cdot\mathbf{k} = (b_1b_2 + b_2b_3 + b_3b_1)^{1/2} = c \end{aligned}\right\}. \quad (5)$$

The nondimensionalization used by Lorenz is

$$\left.\begin{aligned} &\psi = 2L^2f\sum y_i\phi_i \qquad \chi = 2L^2f\sum x_i\phi_i \\ &z = 2f^2L^2g^{-1}\sum z_i\phi_i \quad h = 2f^2L^2g^{-1}\sum h_i\phi_i \\ &F = 2f^3L^2g^{-1}\sum F_i\phi_i \quad t = f^{-1}\tau \end{aligned}\right\}. \quad (6)$$

The resulting equations of the low-order model are

$$a_i\dot{x}_i = a_ib_ix_jx_k - c(a_i - a_k)x_jy_k + c(a_i - a_j)y_jx_k - 2c^2y_jy_k - \nu_0a_i^2x_i + a_i(y_i - z_i), \quad (7)$$

$$a_i\dot{y}_i = -a_kb_kx_jy_k - a_jb_jy_jx_k + c(a_k - a_j)y_jy_k - a_ix_i - \nu_0a_i^2y_i, \quad (8)$$

$$\dot{z}_i = -b_kx_j(z_k - h_k) - b_j(z_j - h_j)x_k + cy_j(z_k - h_k) - c(z_j - h_j)y_k + g_0a_ix_i - \kappa_0a_iz_i + F_i, \quad (9)$$

where $\nu = \nu_0fL^2$, $\kappa = \kappa_0fL^2$, $g_0 = gHf^{-2}L^{-2}$, and Eqs. (7)–(9) are defined for each cyclic permutation of (1, 2, 3); g_0 is the square of the ratio of the Rossby radius of deformation to the horizontal length scale.

Some of the intermediate models are truncations or expansions of the primitive equations based on a Rossby number expansion of the first kind (see McWilliams and Gent, 1980). Requirements of this expansion in Eqs. (6)–(9) are that g_0 is an order 1 quantity independent of the Rossby number, the diffusivities ν_0 and κ_0 are proportional to the Rossby number, and the forcing F_i is proportional to the square of the Rossby number. From hereon we put $\kappa_0 = \nu_0$.

b. *Balance equations (BE)*

The balance equations are truncations of the vorticity and divergence equations. In the vorticity equation the term omitted is a vertical advection term which is identically zero in this model, so that the vorticity equation, along with the height equation, are exact [i.e., Eqs. (8) and (9)]. The divergence equation for constant f is truncated to

$$\nabla\cdot(\nabla^2\psi\nabla\psi) - \tfrac{1}{2}\nabla^2(\nabla\psi\cdot\nabla\psi) + f\nabla^2\psi = g\nabla^2 z, \quad (10)$$

which in the low-order model gives

$$a_iy_i - 2c^2y_jy_k = a_iz_i. \quad (11)$$

c. *Geostrophic momentum (GM)*

The geostrophic momentum approximation replaces the acceleration and diffusion of the total ve-

[2] Mass diffusion, of course, is unphysical. However, height in the shallow water equations is the analog of potential temperature in the atmosphere, which can be diffused. We are grateful to Andrew Bennett for reminding us of this fact.

locity by just those of the geostrophic part of the velocity. Thus the momentum equation becomes

$$\left(\frac{\partial}{\partial t}+\mathbf{V}\cdot\nabla\right)\left(\frac{g}{f}\mathbf{k}\times\nabla z\right)+f\mathbf{k}\times\mathbf{V}$$
$$=-g\nabla z+\nu\nabla^2\left(\frac{g}{f}\mathbf{k}\times\nabla z\right). \quad (12)$$

The low-order forms of the divergence and vorticity equations derived from (12) are

$$a_i(z_i-y_i)+c^2(y_jz_k+z_jy_k)$$
$$-cb_i(z_jx_k-x_jz_k)=0, \quad (13)$$

$$a_i\dot{z}_i+\nu_0a_i^2z_i+a_ix_i+b_i(b_jx_jz_k+b_kz_jx_k)$$
$$-c(b_kz_jy_k-b_jy_jz_k)=0. \quad (14)$$

Eqs. (13) and (14) along with the exact height equation (9) are the geostrophic momentum equations.

d. Hypogeostrophy (HG)

The hypogeostrophic equations are expansions of the governing equations (7)–(9) which are accurate through O(R) in a Rossby number expansion of the first kind. The resulting equations are

$$(1+a_ig_0)\dot{z}_i+\dot{z}_j[z_kg_0(2c^2-a_kb_k)-b_k(z_k-h_k)]$$
$$+\dot{z}_k[z_jg_0(2c^2-a_jb_j)-b_j(z_j-h_j)]$$
$$=F_i-a_i\nu_0(1+a_ig_0)z_i+g_0z_jz_k[c(a_k-a_j)$$
$$-\nu_0a_i(2c^2+a_ja_k)]+c(h_jz_k-h_kz_j)$$
$$+\nu_0[z_j(z_k-h_k)a_jb_k+z_k(z_j-h_j)b_ja_k]$$
$$+c\{z_iz_k(z_k-h_k)(a_i-b_j)$$
$$-z_iz_j(z_j-h_j)(a_i-b_k)+z_iz_k^2g_0(a_kb_k+2b_j^2)$$
$$-z_iz_j^2g_0(a_jb_j+2b_k^2)\}, \quad (15)$$

with

$$a_iy_i=a_iz_i+2c^2z_jz_k, \quad (16)$$

$$a_ix_i=-a_i(\dot{z}_i+\nu_0a_iz_i)-\dot{z}_jz_k(2c^2-a_kb_k)$$
$$-\dot{z}_kz_j(2c^2-a_jb_j)+z_jz_k[c(a_k-a_j)$$
$$-\nu_0a_i(2c^2+a_ja_k)]-cz_iz_j^2(a_jb_j+2b_k^2)$$
$$+cz_iz_k^2(a_kb_k+2b_j^2). \quad (17)$$

e. Linear balance equations (LBE)

The linear balance equations are again truncations of the vorticity and divergence equations as described in Lorenz (1960). The constant-f form of the vorticity equation is

$$\left(\frac{\partial}{\partial t}+\mathbf{k}\times\nabla\psi\cdot\nabla\right)\nabla^2\psi+f\nabla^2\chi=\nu\nabla^4\psi, \quad (18)$$

which in the low-order model reduces to

$$a_i\dot{y}_i=c(a_k-a_j)y_jy_k-a_ix_i-\nu_0a_i^2y_i. \quad (19)$$

The divergence equation retains only linear terms and is

$$f\nabla^2\psi=g\nabla^2z \quad (20)$$

or

$$y_i=z_i. \quad (21)$$

Eqs. (19) and (21) along with the exact height equation (9) are the linear balance equations.

f. Quasigeostrophy (QG)

The quasigeostrophic equations are the leading order terms in a Rossby number expansion of the exact equations (7)–(9). They are

$$(1+a_ig_0)\dot{z}_i=F_i-a_i\nu_0(1+a_ig_0)z_i$$
$$+g_0c(a_k-a_j)z_jz_k+c(h_jz_k-h_kz_j), \quad (22)$$

with

$$y_i=z_i, \quad (23)$$

$$a_ix_i=c(a_k-a_j)z_jz_k-a_i(\dot{z}_i+\nu_0a_iz_i). \quad (24)$$

3. Methods of solution

All models are integrated forward in time using the Taylor series scheme of Lorenz (1980). This consists of evaluating the first four time derivatives of each variable s at time τ and then setting

$$s(\tau+\Delta\tau)=\sum_{p=0}^{4}[d^ps(\tau)/d\tau^p]\Delta\tau^p/p!, \quad (25)$$

where the time increment $\Delta\tau$ is chosen to ensure numerical accuracy to $O(10^{-5})$. PE and QG are straightforward to integrate because each dependent variable has an explicit first-order differential equation in time which can be differentiated $p-1$ times to obtain an expression for $d^ps/d\tau^p$. All the intermediate models, however, have solvability conditions which, in the low-order models, take the form of being able to invert possibly singular matrices. The methods of solving each intermediate model are now described.

a. Hypogeostrophy

The left-hand side of Eq. (15) contains the time derivatives of all three of the model variables z_1, z_2, and z_3. Thus it can be written as

$$\mathsf{A}(\mathbf{z})\dot{\mathbf{z}}=B(\mathbf{z}), \quad (26)$$

where A is a 3×3 symmetric matrix which is a function of the variables z_i, and $\mathbf{z}$ and $B(\mathbf{z})$ are column vectors containing three elements. To solve Eq. (26) for $\dot{\mathbf{z}}$ requires inverting the matrix A, as does

solving differentiated forms of (26) for higher derivatives of **z**, so that this is the solvability condition for hypogeostrophy. Note that in this model, as in quasigeostrophy, the heights z_i are the basic variables, and the rotational streamfunction and velocity potential are calculated diagnostically.

b. Linear balance equations

Eqs. (9), (19) and (21) can be combined into a single equation which is

$$\begin{aligned}(1 + a_ig_0)\dot{z}_i - b_k\dot{z}_j(z_k - h_k) - b_j\dot{z}_k(z_j - h_j)\\ = F_i - \nu_0 a_i(1 + a_ig_0)z_i + h_jz_k(c - \nu_0 a_kb_j)\\ - z_jh_k(c + \nu_0 a_jb_k) + z_jz_k[cg_0(a_k - a_j)\\ + \nu_0(a_jb_k + a_kb_j)] - cb_j(a_j - a_i)z_iz_j(z_j - h_j)/a_k\\ + cb_k(a_k - a_i)z_iz_k(z_k - h_k)/a_j. \quad (27)\end{aligned}$$

Thus, the LBE can be solved analogously to hypogeostrophy with the solvability condition being the inversion of a somewhat simpler 3×3 symmetric matrix and the streamfunction and potential being calculated diagnostically from Eqs. (21) and (19).

c. Geostrophic momentum

Two of the geostrophic momentum equations [(9) and (14)] are prognostic equations for the height z_i. These can be subtracted to give the diagnostic equation

$$\begin{aligned}a_i(1 + a_ig_0)x_i + x_j[z_k(b_ib_j - a_ib_k) + a_ib_kh_k]\\ + x_k[z_j(b_ib_k - a_ib_j) + a_ib_jh_j] - cy_j(b_kz_k + a_ih_k)\\ + cy_k(b_jz_j + a_ih_j) + a_iF_i = 0. \quad (28)\end{aligned}$$

Eqs. (13) and (28) are diagnostic equations which can be used to determine x_i and y_i for given values of z_i. This involves inverting a nonsymmetric 6×6 matrix which is a function of **z**; this is the geostrophic momentum solvability condition. The heights z_i can then be advanced using either Eqs. (9) or (14).

d. Balance equations

The diagnostic equation (11) can be differentiated to give

$$a_i(\dot{y}_i - \dot{z}_i) - 2c^2(y_j\dot{y}_k + \dot{y}_jy_k) = 0. \quad (29)$$

Substitution from Eqs. (8) and (9) gives the diagnostic equation for x_i:

$$\begin{aligned}x_i[a_ia_ja_k(1 + g_0a_i) - 2c^2(a_j^2b_jy_j^2 + a_k^2b_ky_k^2)]\\ - x_j[a_ja_k\{y_k(2c^2 - a_kb_k) + a_ib_k(z_k - h_k)\}\\ + 2c^2a_ia_jb_iy_iy_j] - x_k[a_ja_k\{y_j(2c^2 - a_jb_j)\\ + a_ib_j(z_j - h_j)\} + 2c^2a_ia_kb_iy_iy_k]\\ = a_ja_k[c(a_k - a_j)y_jy_k + ca_i\{(z_j - h_j)y_k\\ - y_j(z_k - h_k)\} + a_i\{\nu_0a_i(z_i - y_i) - F_i\}]\\ - 2c^2[ca_j(a_j - a_i)y_iy_j^2 + ca_k(a_i - a_k)y_iy_k^2\\ - \nu_0a_ja_k(a_j + a_k)y_jy_k]. \quad (30)\end{aligned}$$

To solve the balance equations the easiest basic variable to work with is the rotational velocity streamfunction. For given values of y_i, the heights z_i are first found from the diagnostic equation (11). Then the values of x_i are found from Eq. (30) by inverting a very complicated nonsymmetric 3×3 matrix which is a function of both **y** and **z**; this is the balance equation solvability condition. y_i is then advanced in time using Eq. (8) and, as an internal numerical model check, z_i also can be advanced in time using Eq. (9) and compared to the values found by using Eq. (11). If the balance equations are to be initialized using given initial values of the height field, then Eq. (11) has to be inverted once and only once to determine the initial **y** values from the given initial **z** values. This requires solving a fifth-order polynominal for y_i, which is difficult to analyze in general. In practice, a simple iteration scheme quickly converged using $z_i(0) + 2c^2z_jz_k(0)/a_i$ as the initial guess for y_i.

After some initial work with alternate parameter values (see Section 5), we reverted to those used by Lorenz (1980). They are

$$\left.\begin{aligned}f^{-1} = 3\text{ h}, \quad g = 10\text{ m s}^{-2}\\ H = 8\text{ km}, \quad L = 1080\text{ km}\\ |h| = 2\text{ km}, \quad \nu = \kappa = 2.25 \times 10^6\text{ m}^2\text{ s}^{-1}\end{aligned}\right\}, \quad (31)$$

which imply a six-day diffusive damping time for 1 and 2 subscripted variables and a two-day damping time for subscript 3 variables. Thus the values of the nondimensional parameters used are

$$\left.\begin{aligned}g_0 = 8, \quad \nu_0 = \kappa_0 = {}^1\!/_{48}\\ a_1 = a_2 = 1, \quad a_3 \equiv a = 3\\ h_1 = -1, \quad h_2 = h_3 = F_2 = F_3 = 0\end{aligned}\right\}, \quad (32)$$

where the topography and forcing are only in the direction of ϕ_1. The models were then run at different values of the forcing F_1, the square root of which can be interpreted as the Rossby number. The time steps used for most of the calculations were 15 min ($\Delta\tau = {}^1\!/_{12}$) for the primitive equations and 3 h ($\Delta\tau = 1$) for all the other models where there are no gravity waves. In order to ensure numerical accuracy and stability, these time steps had to be reduced for both the smallest and largest values of F_1 used.

4. Model comparisons

The regimes of behavior found in all the models are displayed in Fig. 1, and the values of the forcing

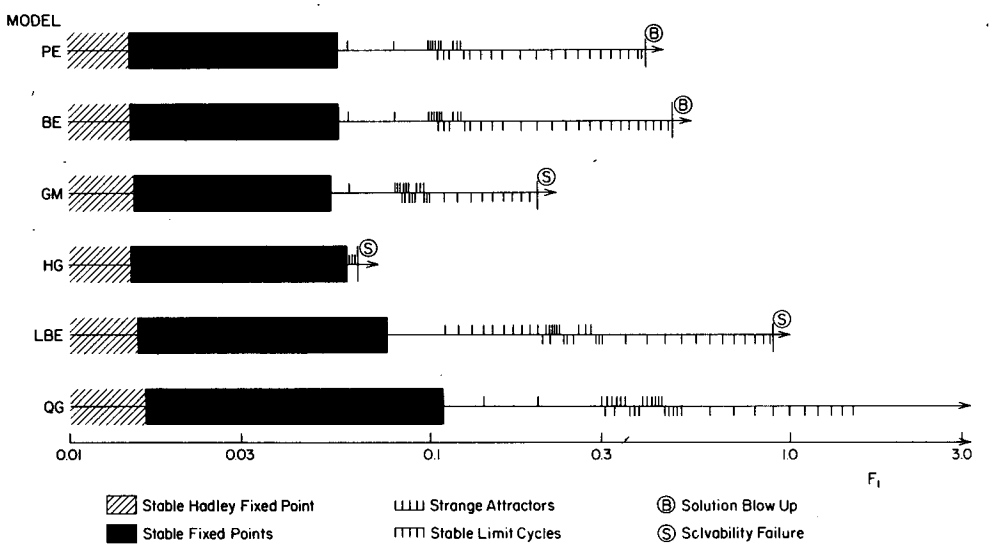

FIG. 1. Regimes of model behavior.

F_1 at regime transitions are listed in Table 1. The regimes and transitions are discussed below.

The PE possess a fixed point in which the flow is purely zonal and nearly geostrophic which Lorenz describes as the Hadley circulation. It is given by

$$\left.\begin{aligned} x_1 &= -\nu_0 a_1 y_1, \\ y_1 &= F_1/a_1\nu_0(1 + a_1 g_0 + \nu_0^2 a_1^2) \\ z_1 &= (1 + \nu_0^2 a_1^2) y_1 \\ x_2 = x_3 = y_2 = y_3 = z_2 = z_3 &= 0 \end{aligned}\right\}. \quad (33)$$

The corresponding Hadley fixed point in the BE is

$$y_1 = F_1/a_1\nu_0(1 + a_1 g_0), \quad y_2 = y_3 = 0, \quad (34)$$

and in all the other models is

$$z_1 = F_1/a_1\nu_0(1 + a_1 g_0), \quad z_2 = z_3 = 0. \quad (35)$$

For very small values of F_1, this Hadley fixed point is stable. Its stability was tested by starting with initial conditions very close to (33)–(35) (i.e., with $y_2 = -z_2 = -10^{-5}$ for PE, $y_2 = -10^{-5}$ for BE and $z_2 = 10^{-5}$ for the other models). These are the initial conditions used in most of the numerical integrations described in this section, but some runs also were made where all variables were set initially to 0.1. The values of F_1 where the Hadley fixed point becomes unstable are listed in Table 1 correct to four significant figures. In fact, the QG value can be determined analytically and occurs when r, which is defined in Eq. (53) of Lorenz (1980), equals 1 (see Lorenz, 1963). The two intermediate models which are correct through order Rossby number in a quasigeostrophic ordering of the first kind are BE and HG (see McWilliams and Gent, 1980), and, at these very small values of F_1, these two models have their transitions closest to the PE one. GM and LBE are only correct through leading order, but their transition values are considerable improvements over the QG value which also is correct at leading order.

As F_1 is increased, all models possess at least two other stable fixed points in which the 2 and 3 subscripted variables are nonzero. When these fixed points become unstable all models change over to a

TABLE 1. Values of F_1 at regime transitions.

Model	Hadley fixed point becomes unstable	Apparent transition T to strange attractors	Range of interleaving between strange attractors and stable limit cycles*	Upper limit of forcing	Reason for breakdown
PE	0.01494	0.0516	0.106–0.123	0.40	Blow-up
BE	0.01494	0.0516	0.106–0.123	0.47	Blow-up
GM	0.01513	0.0482	0.084–0.096	0.20	Solvability
HG	0.01487	0.0546	—	0.063	Solvability
LBE	0.01540	0.0710	0.205–0.280	0.90	Solvability
QG	0.01630	0.1031	0.307–0.448	∞	—

* These values are only approximate and not exact, see Section 4.

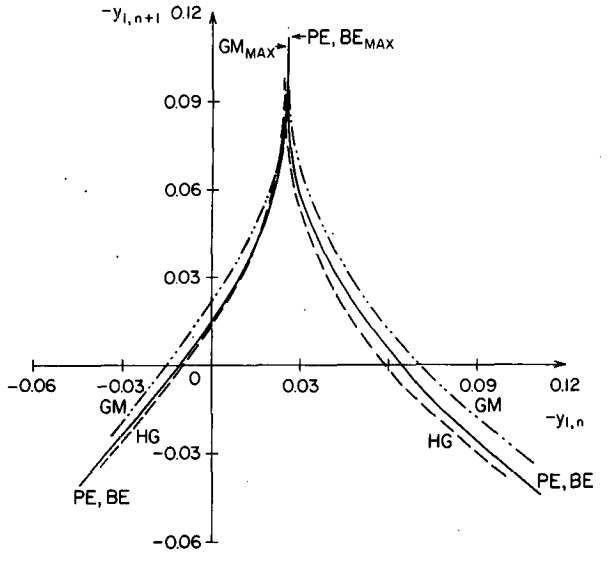

FIG. 2. Successive minima maps of the PE, BE, GM and HG models when $F_1 = 0.06$.

regime of strange attractors. For QG the fixed points and transition are known analytically (see Lorenz, 1963); the transition to strange attractors occurs when $r = 21$ or $F_1 = 0.10785$. This transition to strange attractor is reasonably difficult to quantify in the other models because, as the transition is approached from the stable side, an increasingly long integration time is needed before the solution passes close enough to the stable fixed point that it is attracted to it. Thus we estimated the transition T by another method using successive minima maps. The models' strange attractors have the property that the value of y_1 at one minimum is a nearly perfect predictor of the value at the following minimum. A plot of values of y_1 minima against the previous y_1 minimum is shown in Fig. 5 of Lorenz (1980) for the PE model with $F_1 = 0.1$ (note that Lorenz defines $Y_i = -a_i y_i$). In his Fig. 10, Lorenz shows successive minima maps for the QG model when $F_1 = 0.1$, 0.15 and 0.2; note that for $F_1 = 0.1$ stable fixed points exist although this is not immediately apparent from the successive minima map (it is drawn from an initial transient phase before the solution spirals into the fixed point). If an integration is started at the Hadley fixed point then the value of the first minimum of y_1 is the cusp in the successive minima map (see Lorenz, 1980), and for maps near the transition the next minimum of y_1 has its largest positive value (i.e., there is no local minimum in the successive minima map for QG with $F_1 = 0.1$ or the maps shown in Fig. 2 where the values of F_1 are slightly above the transition values). If succeeding y_1 minima decrease in magnitude the solution acts like a strange attractor; if they increase in magnitude the solution slowly spirals into a stable fixed point. We define the apparent transition T_a as the value of the forcing such that succeeding minima of y_1 remain constant when starting from initial conditions near the Hadley fixed point. T_a is always an underestimate of the true transition T. The values of T_a for all the models are listed in Table 1; they are accurate to $\pm 10^{-4}$. For the QG model,

$$T = T_a + 0.0047, \tag{36}$$

and this is the formula we used to estimate T from T_a for the other models. Those values, truncated to two significant figures, are the ones plotted in Fig. 1. The difference between T and T_a is probably a function of the value of F_1 at the transition, but the values of T_a for GM and HG both differ from the PE value by $\sim 6\%$ so that the conclusion, that GM and HG are comparable in accuracy compared to PE at this transition, is not invalidated by this functional dependence. The BE model is still extremely accurate at this transition, and again the LBE value is a considerable improvement over the QG value.

Fig. 2 shows the successive minima maps for those models that have strange attractors when $F_1 = 0.06$. In this figure, and all subsequent ones, the PE and BE curves differ by less than the thickness of the lines. The figure shows that there is little to choose between GM and HG at this value of F_1 in that the HG curve is generally closer to the PE one but GM gets the cusp location somewhat better than HG. Fig. 3 shows the initial escape from the Hadley fixed point in the phase space of y_2 and y_3 for the same models. The parts of the curves with positive y_3 represent the outer boundary of the respective strange attractors (see Lorenz, 1980, Figs. 6 and 7), and in general the HG shape is slightly closer than GM to the PE shape.

When $F_1 = 0.063$ the HG calculation starting from the Hadley fixed point has a solvability failure in that its solution matrix cannot be inverted. This means that HG has very quickly gone awry because it is a reasonably good approximation to PE at $F_1 = 0.06$. Its behavior becomes implausible and very different from all the other models when F_1 is slightly larger because the Hadley fixed point becomes stable again when $F_1 \geqslant 0.074$; no other model exhibits this behavior.

As F_1 is increased further in the other models, stable limit cycles begin to be encountered. Regions of stable limit cycles and strange attractors are then interleaved until, at higher values of F_1, only stable limit cycles are found (see Fig. 1). In each model the limit cycles increase in complexity and occur in narrower bands of F_1 as the value of the forcing is decreased. The most complicated limit cycle found is in GM for $F_1 = 0.084$ when y_1 and y_2 go through zero 40 and 26 times, respectively, during each cycle. We have by no means delineated all the complex interleaving behavior between strange attractors and stable limit cycles in any model, but Fig. 1 and Table

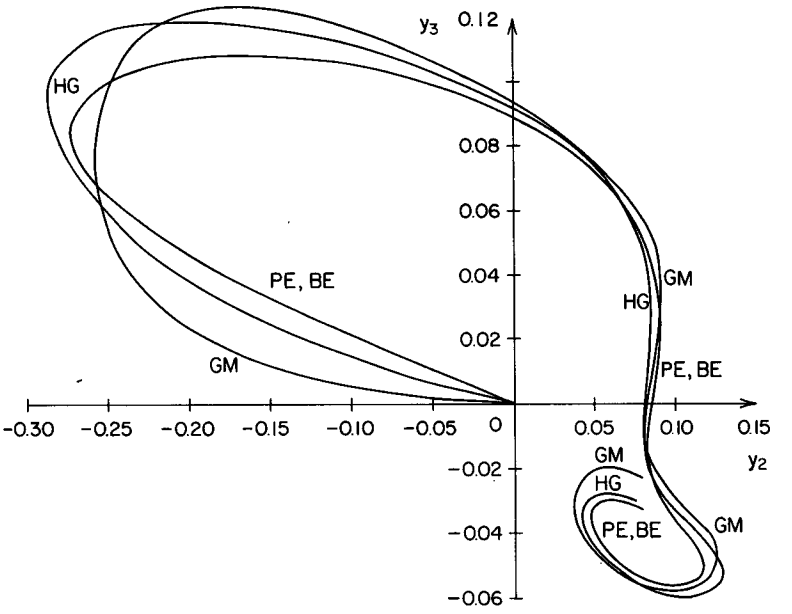

FIG. 3. Orbits from the Hadley fixed point projected onto the y_2, y_3 plane for the PE, BE, GM and HG models when $F_1 = 0.06$.

1 show this interleaving well enough for comparison purposes. BE is still excellent at reproducing the PE results (the first time PE and BE behavior are noticeably different is when $F_1 = 0.24$), GM is fairly good, and LBE is still a considerable improvement over QG. This feature of interleaving in a transition from only strange attractors to only limit cycles has been seen previously in a low-order model equivalent to QG here (Pedlosky and Frenzen, 1980).

As illustrative of this type of behavior, we have made a model comparison when $F_1 = 0.1$. PE, BE and LBE have strange attractors at this forcing value, and their successive minima maps are shown in Fig. 4. QG has stable fixed points when $F_1 = 0.1$, but the comparable map of an initial transient phase of a QG solution is given in Fig. 10 of Lorenz (1980). The cusp is at $-y_{1n} \approx 0.9$ in QG, as compared to ≈ 0.8 in LBE and ≈ 0.6 in PE and BE. The escape of PE, BE and LBE solutions from the Hadley fixed point at $F_1 = 0.1$ is plotted in Fig. 5 in the phase space of y_2 and y_3; again for $y_3 > 0$ this delineates the outer edge of the respective strange attractors. At this forcing GM has a stable limit cycle and its projection onto the y_2 and y_3 plane is also plotted in Fig. 5. The cycle is a relatively simple one, with y_1 and y_2 going through zero four times and twice, respectively.

As the forcing is increased further, the PE and BE solutions finally diverge to infinity (this is possible because the models do not have positive definite energy conservation principles—see the Appendix). The HG, GM and LBE models have solvability failures at the values of F_1 given in Table 1. The QG model does have energy and enstrophy conservation principles. It can be shown from Eq. (22) that

$$\frac{d\epsilon}{d\tau} = \sum_i z_i[F_i g_0^{-1} - \nu_0 a_i(a_i + g_0^{-1})z_i], \quad (37)$$

where

$$\epsilon = \sum_i \tfrac{1}{2}(a_i + g_0^{-1})z_i^2, \quad (38)$$

$$\frac{dQ^2}{d\tau} = 2\sum_i [a_i z_i + g_0^{-1}(z_i - h_i)] \times [F_i g_0^{-1} - \nu_0 a_i(a_i + g_0^{-1})z_i], \quad (39)$$

$$Q^2 = \sum_i [a_i z_i + g_0^{-1}(z_i - h_i)]^2. \quad (40)$$

We have nondimensionalized energy and enstrophy here by $2HL^2f^2$ and $2Hf^2$, respectively. Thus the QG solution cannot diverge to infinity because, for any F_i the right-hand sides of (37) and (39) become negative for large enough z_i and this bounds ϵ and Q^2. Furthermore, there is no QG solvability condition, and solutions can be obtained for all F_1 values.

Finally, we offer two comments about behavior that is peculiar to the PE model. First, for the larger forcing values, $0.25 < F_1 < 0.4$, the solutions appear to be almost but not quite, stable limit cycles (as shown in Fig. 1) in that the solution seems to follow a slightly different orbit in phase space in each cycle. It appears that the gravity waves do not die when the forcing is strong but modulate the stable limit cycle of the Rossby wave component of the solution. Second, the PE has a set of stable fixed points that

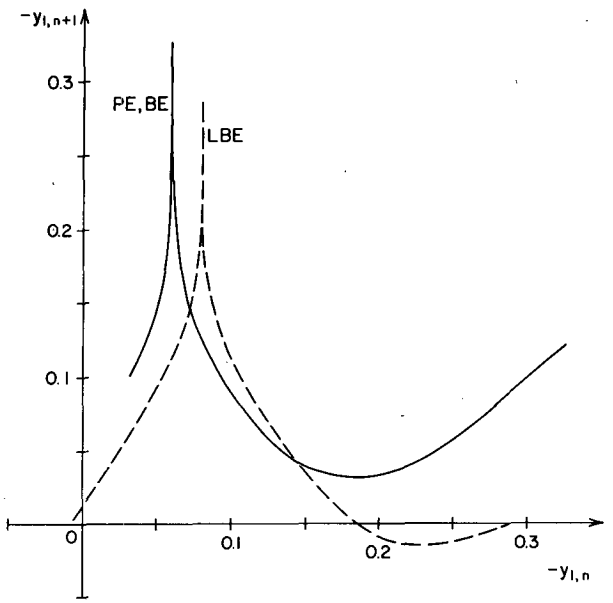

FIG. 4. Successive minima maps of the PE, BE and LBE models when $F_1 = 0.1$.

no other model possesses. When $F_1 = 0$ the fixed point is

$$\left.\begin{aligned} x_1 &\approx -x_2 = 4.80 & x_3 &= -0.05 \\ y_1 &\approx y_2 = 0.55 & y_3 &= 0.59 \\ z_1 &= -5.32, \quad z_2 = -4.32, & z_3 &= -14.10 \end{aligned}\right\} . \quad (41)$$

The fixed point is far from being geostrophic; in Eq. (7), the main contribution to z_3 comes from $b_3x_1x_2$ which is a term neglected in all the other models. The stable fixed point values of (41) are insensitive to the value of F_1 as it is varied in the range $0 \leqslant F_1 \leqslant 0.5$. This is the only situation where we found a dependence of the final solution upon the initial conditions chosen; that is, the PE can either approach (41) or the solutions in Fig. 1, depending on initial conditions.

5. Caveats

Whether or not an intermediate model possesses integral invariants may be important in assessing the quality of models, especially well away from asymptotic limits (see McWilliams and Gent, 1980). It is shown in the Appendix that 1) the HG, BE and LBE models do not have an energy conservation principle in the shallow water equations, and 2) of the remaining models only QG retains its energy conservation principle when cast in the triad truncation formulation of the Lorenz model. All of the models except HG have enstrophy conservation principles in the shallow water equations; but again only that of QG persists in triad truncation. Our position on integral invariants is that it is reassuring when equations have them and computational techniques should conserve them whenever possible. However, we feel that if an equation set does not have certain integral invariants this does not invalidate using it in many

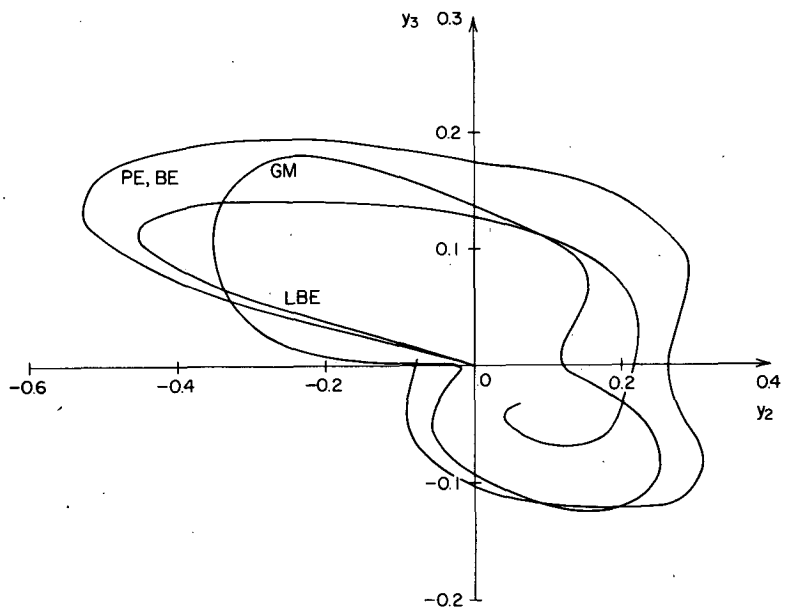

FIG. 5. Projections onto the y_2, y_3 plane of the orbits from the Hadley fixed point for the PE, BE and LBE models and the stable limit cycle of the GM model when $F_1 = 0.1$.

contexts (e.g., with strong forcing and damping) provided sufficient caution is used. This lack of integral invariants in all low-order models except QG means that the intermediate Lorenz model comparison at large values of F_1 should be viewed with some reservation. The slightly peculiar PE behavior for $0.25 < F_1 < 0.4$ that was noted in Section 4 may possibly be linked to the lack of an energy conservation principle, and certainly occurs close to the PE blow up.

The second caveat concerns PE and QG solution convergence as the forcing, or equivalently the Rossby number, is reduced. If the values of ν_0, κ_0 and h_1 from (32) are all reduced by a factor n, then the analytic QG transition to strange attractors (T_{QG}) occurs when F_1 is reduced by a factor n^2 (i.e., the Rossby number is reduced by a factor n). The ratio of the forcing at the QG transition to that of the PE transition was calculated for several successively larger reductions of these parameters until a consistent two-term asymptotic formula was found for the ratio. This procedure was also followed for two alternate sets of the dimensional parameters (31). These had for g_0, which is the square of the ratio of the Rossby radius of deformation to the horizontal length scale, the values 2 and ½, which are certainly not geophysically unreasonable. The results can be broadly summarized by

$$T_{QG}/T_{PE} \approx 1 + R, \quad \text{for} \quad R \leqslant 1,$$
$$\text{where} \quad R = 32 F_1^{1/2} g_0^{-1}, \qquad (42)$$

and F_1 is the forcing value at the PE transition. For example (42) gives the ratio as almost 2 for the Lorenz parameters. Thus, the PE and QG solution convergence appears to be governed by an equivalent Rossby number R and not the obvious Rossby number $F_1^{1/2}$. These two Rossby numbers can differ by two orders of magnitude for the not unreasonable value of $g_0 = ⅓$, so that convergence in the Lorenz model can be extremely slow. Even when $g_0 = 8$, as in (31), the two differ by a factor of 4, so that solution convergence is about four times slower than expected based on a Rossby number of $F_1^{1/2}$. This should be borne in mind when making quantitative comparisons from Table 1, for example.

6. Conclusions

From the results of Section 4, the following ranking, from best to worst, of the models can be made:

Small Rossby number:

PE, BE, HG, GM, LBE, QG.

Intermediate Rossby number:

PE, BE, GM, LBE, QG, HG.

This ranking is exactly the same as that from the steady circular flow comparison in McWilliams and Gent (1980) (n.b., the LBE and QG as well as the PE and BE models are identical for steady circular flow). It is encouraging that in two different moderately geostrophic situations with different physical processes the intermediate models have the same ranking. Even QG is a very good analogue model to PE in both these circumstances in the sense that it is simpler and is qualitatively correct, in that it retains the same phenomenology, although it is quantitatively incorrect. Intermediate models are attempts to obtain better quantitative accuracy, but this should not be at the expense of losing analogues of PE physical behavior; this loss at intermediate Rossby number (i.e., no stable limit cycles were found) is a serious disadvantage of HG. As the Rossby number becomes large, QG can only improve its ranking in the sense that all other intermediate models may have a solvability failure. In this comparison, however, only HG and GM have solvability failures at small enough values of the forcing to be judged deficient in this regard. This loss of analogues of PE physical behavior and the apparently small radius of convergence in Rossby number of the asymptotic expansion (both here and for steady circular flow) indicate that HG probably should not be recommended as an intermediate model.

Perhaps the most surprising result of this study is that the BE are so accurate compared to the PE. Lorenz (1980) defines the unknown equation describing the invariant manifold of the PE as the superbalance equation, which only has three degrees of freedom in this low-order truncation. An empirical conclusion of our study is that, for small or medium values of the forcing, the BE are virtually indistinguishable from the superbalance equation. Thus, in this model the rate of change of the divergent rather than the ageostrophic velocity remains small as the Rossby number is increased. This identification cannot be made with certainty when the forcing is large because the PE solutions appear to retain some gravity waves (i.e., the manifold has more than three degrees of freedom) and because of the proximity in Rossby number to the divergence to infinity of both PE and BE solutions. Why are the BE so good? We only have suggestions: gravity waves are a known contaminent of many PE solutions; they are most directly characterized by their divergent accelerations, and the neglect of this term is the underlying basis for the BE approximation (rather than neglecting the ageostrophic velocity acceleration as in GM); BE is the only order Rossby number accurate model that retains some of the PE global invariants (HG has no global invariants).

There are a number of caveats to the generality of these conclusions. The Lorenz model does not al-

low a frontal asymptotic comparison to be made and, for example, it is shown in McWilliams and Gent (1980) that BE will probably not be nearly so accurate in this situation. We also feel uncomfortable about the fact that the Lorenz model does not have integral invariants that are physically correct for the shallow water equations (i.e., energy and enstrophy). The slow Rossby number convergence of the low-order models illustrated by Eq. (42) is contrary to our intuition when geophysically relevant parameters are used. However, perhaps our intuition about PE and QG convergence as the Rossby number tends to zero should be questioned. Finally, behavior in very low-order models, such as strange attractors as a simple analogue of turbulence, may not be retained as the order increases indefinitely and the model becomes more exact. However, Curry (1978) has shown that strange attractors still occur when the three-component QG model is generalized to one having 14 components.

Acknowledgment. We would like to thank Ed Lorenz for stimulating discussions about his work and for sharing with us his PE and QG numerical models.

APPENDIX

Energy Conservation

1. The primitive equations

The PE for the unforced, inviscid, adiabatic shallow-water equations over a flat bottom [Eqs. (1) and (2) with $\nu = \kappa = F = h = 0$] can be manipulated to show the conservation of total energy:

$$\frac{d\epsilon_{PE}}{dt} = 0, \tag{A1}$$

where

$$\epsilon_{PE} = \frac{1}{2}\int\int dxdy[(H + z)\mathbf{V}^2 + gz^2] \tag{A2}$$

and the horizontal domain is assumed periodic in x and y.

2. The quasigeostrophic equations

The counterpart of the above for QG is

$$\epsilon_{QG} = \frac{1}{2}\int\int dxdy[H(gf^{-1}\nabla z)^2 + gz^2]. \tag{A3}$$

3. The intermediate models

One of the intermediate models under consideration has a conserved energy, but the other three do not. For GM the energy is

$$\epsilon_{GM} = \frac{1}{2}\int\int dxdy[(H + z)(gf^{-1}\nabla z)^2 + gz^2]. \tag{A4}$$

For HG there is no conserved ϵ, but this is to be expected for a model derived as a truncated asymptotic expansion, when more terms than the leading order ones are retained (McWilliams and Gent, 1980). For BE and LBE there are also no conserved energies. This fact is somewhat surprising, however, since both of these models do have a conserved energy for either a barotropic or continuously stratified fluid contained between rigid and flat upper and lower boundary surfaces (Lorenz, 1960).

By analogy with the energy forms for PE, QG and GM, as well as the kinetic energy density $\nabla\psi\cdot\nabla\psi/2$ for the BE and LBE in a continuously stratified fluid, we select the following as the most plausible candidates for conserved energies in BE or LBE:

$$\left.\begin{aligned}\epsilon_1 &= \frac{1}{2}\int\int dxdy[H\nabla\psi\cdot\nabla\psi + gz^2]\\ \epsilon_2 &= \frac{1}{2}\int\int dxdy[(H + z)\nabla\psi\cdot\nabla\psi + gz^2]\end{aligned}\right\}. \tag{A5}$$

It can be shown, however, that neither of these forms is conserved. In the LBE, for example,

$$\left.\begin{aligned}\frac{d\epsilon_1}{dt} &= g\int\int dxdyz\nabla z\cdot\nabla\chi\\ \frac{d\epsilon_2}{dt} &= \int\int dxdy(H + z)\nabla\chi\cdot\nabla[\tfrac{1}{2}\nabla\psi\cdot\nabla\psi]\end{aligned}\right\}. \tag{A6}$$

Thus there is a basic energetic inconsistency between the BE and LBE vorticity and divergence equation truncations and a deforming free surface of the fluid layer.

4. Low-order truncation

When the continuous PE are projected onto the wave triad of the Lorenz model, the total energy (A2) takes the form

$$\epsilon_{PE} = \sum_i \tfrac{1}{2}[a_i(x_i^2 + y_i^2) + g_0^{-1}z_i^2] - g_0^{-1}z_i[c(y_jx_k - y_kx_j) + b_i(x_jx_k + y_jy_k)]. \tag{A7}$$

An equation for the evolution of ϵ_{PE} can be determined from the triad equations (7)–(9) under the assumptions stated in Section 1 of the Appendix. The result is

$$\frac{d\epsilon_{PE}}{d\tau} = -g_0^{-1}\sum_i c(x_jx_k + y_jy_k)(a_jy_jz_k - a_ky_kz_j) + b_i(a_jy_jz_k - a_ky_kz_j)(x_jy_k - x_ky_j). \tag{A8}$$

Thus, in the triad truncation, ϵ_{PE} is no longer conserved. Note that the non-conservative terms in (A8) are all fourth order in amplitude; their cancellation in a continuous energy equation involves interactions

outside any single triad of wavenumbers, and hence they are residual in the Lorenz model.

This failure of cancellation in triad truncation occurs for any integral invariant which is more complicated than a quadratic function of the amplitude variables. Thus, ϵ_{GM} from (A4) is also not conserved in the Lorenz model.

Only ϵ_{QG} from (A3) satisfies the criterion for conservation in a triad model [it is listed in Eq. (38)]. Hence, all of the intermediate models under consideration, as well as PE, do not have an energy conservation principle in the low-order Lorenz model.

REFERENCES

Curry, J. H., 1978: A generalized Lorenz system. *Comm. Math. Phys.*, **60,** 193–204.

Lorenz, E. N., 1960: Energy and numerical weather prediction. *Tellus*, **12,** 364–373.

——, 1963: Deterministic nonperiodic flow. *J. Atmos. Sci.*, **20,** 130–141.

——, 1980: Attractor sets and quasigeostrophic equilibrium. *J. Atmos. Sci.*, **37,** 1685–1699.

McWilliams, J. C., and P. R. Gent, 1980: Intermediate models of planetary circulations in the atmosphere and ocean. *J. Atmos. Sci.*, **37,** 1657–1678.

Pedlosky, J., and C. Frenzen, 1980: Chaotic and periodic behavior of finite-amplitude baroclinic waves. *J. Atmos. Sci.*, **37,** 1177–1196.